Proc. of SPIE Vol. 1533, Optomechanics and Dimensional Stability, ed. R A Paquin, D Vukobratovich (Dec 1991) Copyright SPIE

Rapid Cooled Lens Cell

David M. Stubbs
Ike C. Hsu

Lockheed Research & Development Division
3251 Hanover St., Palo Alto, CA 94304-1187

ABSTRACT

This paper describes the opto-mechanical design, thermal analysis, fabrication, and test evaluation processes followed in developing a rapid cooled, infrared lens cell. Thermal analysis was the key engineering discipline exercised in the design phase. The effect of thermal stress on the lens, induced by rapid cooling of the lens cell, was investigated. Features of this lens cell that minimized the thermal stress will be discussed in a dedicated section. The results of thermal analysis on the selected lens cell design and the selection of the flow channel design in the heat exchanger will be discussed.

Throughout the paper; engineering drawings, illustrations, analytical results, and photographs of actual hardware help acquaint the reader with the design. The aim of this paper is to pass on lessons learned in all phases of developing this unique optical component.

2. INTRODUCTION

The Lockheed Research and Development Division (R&DD) is currently under contract with the U.S. Army to develop and test state-of-the-art seeker technology on the Longwave Infrared Advanced Technology Seeker (LATS) program. Requirements for the next generation of infrared seekers are calling for optics which can be rapidly cooled to cryogenic temperatures. These optics must also maintain steady state temperatures throughout the flight envelope with little to no thermal gradients. The engineering challenges in building such systems are formidable.

On the LATS program, Lockheed R&DD has designed, built, and tested a rapid cooled, infrared lens cell. Liquid nitrogen, flowing through an integral heat exchanger, cools the lens cell from 300 K to less than 120 K in under five minutes. The cell housing does not induce stresses in the lens.

A phase change material (PCM) compartment was designed into the lens cell housing for traceability to a future lens cell design which will passively maintain the cell at its cryogenic operating temperature up to twenty five minutes. The lens cell has a 26.0 mm. clear aperture and a mass of 0.37 kg.

3. LENS CELL REQUIREMENTS

The requirements for the lens cell were straightforward. The lens shall be made out of germanium. The entire cell shall rapidly cool from 300 K to 120 K in under five minutes. The cell housing may not induce any stresses into the lens plus maintain dimensional stability. Finally, a phase change material (PCM) compartment shall be designed into the cell housing. The PCM compartment was only an empty volume in this design phase. Future cells will have the added complexity of additional plumbing for PCM injection.

4. PARAMETERS GOVERNING THE THERMAL DESIGN OF THE LENS CELL

The thermal requirement for the lens cell was to rapidly cool the refractive lens element from ambient, 300 K, to 120 K within five minutes. The refractive lens element could not be cooled directly by internal coolant flow. The approach was to cool the lens from its periphery in order not to block the transmission of LWIR radiation. This required the lens element to be housed inside a heat exchanger with coolant circulating through its internal flow channels. The cooling of the lens element is accomplished by conduction through the lens material and the lens/cell housing interface; then by forced convective cooling with a cooling fluid flowing through the cell housing heat exchanger. In order to achieve rapid cooling of the lens element, the following parameters had to be maximized:

1. The thermal diffusivity of the lens material.
2. The contact conductance at the interface between the lens element and the lens cell housing.
3. The surface area in the heat exchanger within the lens cell housing.

The effect of each of these parameters will be discussed in the following paragraphs.

4.1 Thermal diffusivity of the lens material

The thermal diffusivity of a material is defined as:

$$\alpha = k/(\rho\, c_p) \tag{1}$$

This parameter is a combination of physical properties of the lens material, with k as the thermal conductivity, ρ is the density, c_p is the specific heat and α has the unit of cm^2/sec. For rapid cooling, the material with the highest value of α over the temperature range of interest should be preferred. For comparison, the values of α for the two candidate lens materials, germanium (Ge) and zinc selenide (ZnSe) are plotted on Fig. 1. Germanium exhibited a higher value of α over the range of temperature of interest for rapid cooling and was selected as the baseline material for the lens.

4.2 Contact conductance at the interface

When the thermal contact conductance between the back surface of the lens and the cell housing heat exchanger is to be maximized, the contact pressure exerted on the lens must be optimized. Differential thermal contraction of the contacting materials must be minimized at the same time. These conflicting requirements have to be balanced in order to achieve rapid cooling of the lens element without exerting excessive mechanical stress on the lens. The approach taken in this design was to match the coefficient of thermal expansion (CTE) of the two mating materials and maximize the interfacial contact surface area. Molybdenum was chosen for the cell housing (CTE of 5.5 ppm/K), to match the germanium lens (CTE of 4.9 ppm/K). Furthermore, the cell housing interfacial surface was ground and polished, using test plates, to assure the spherical radius matched the COLD (120 K) mating germanium lens radius within two fringes at 3.39 microns.

4.3 Surface area in the heat exchanger

The internal surface area for the flow channels must be maximized in order to enhance the convective heat transfer between the cooling fluid and the housing. The baseline cooling fluid selected for rapid cooling of the lens cell was liquid nitrogen. However, by maximizing the internal surface area or the number of flow channels in the heat exchanger, the flow loss experienced by the liquid nitrogen would increase correspondingly. Since the supply pressure of liquid nitrogen from its dewar is usually maintained at 20 psig, there is a trade-off between the number of flow channels and the flow loss in the heat exchanger. In order to optimize the heat transfer surface area inside the heat exchanger, a detailed thermal analysis of the lens cell design was performed using the SINDA thermal analysis computer code. The thermal model assumed a single phase fluid flowing through the flow channels, cooling the wall surfaces. Any effect due to two phase boiling heat transfer to the liquid nitrogen coolant was not incorporated. The parametric trade study performed using the thermal model varied the number of flow channels from one to ten in the heat exchanger and the results are plotted in Fig. 2 as temperature of the lens housing against time. From these results, there was no advantage in increasing the number of flow channels to more than three in the heat exchanger.

5. TEST CELL DESIGN

A test cell was fabricated for design risk reduction and thermal model validation. Technical issues had to be resolved before committing to a final lens cell design; coolant flow rate, lens heat transfer rate, lens mechanical integrity, and optical changes in the lens and its coatings. All features, sizes and materials in the test cell were identical to the proposed lens cell except for two items. The test cell had a plano element (test flat) installed instead of a lens; for ease of interferometrically testing thermally induced stresses. Secondly, the simulated PCM compartment was deleted due to fabrication cost considerations. Refer to the cross-sectional drawing in Figure 3.

The purchased test flat was manufactured out of germanium. The flatness was specified to $\lambda/10$ for a wavelength of 3.39 microns. An anti-reflecting coating was also specified for both optical surfaces.

Molybdenum was chosen for the housing material due to its closely matched coefficient of thermal expansion (CTE) with germanium; germanium (4.9 ppm/K), molybdenum (5.5 ppm/K). A microfinish surface polish requirement of eight was placed on the housing surface contacting the test flat to assure a good thermal interface.

A flow channel was machined into the housing's outer cylindrical surface. Radial grooves where machined at both ends of the housing to hold the braze material. A cylindrical plenum cover was then brazed over the exposed flow channel. Fill/vent lines were radially brazed to the cover.

Two spring wave washers were used in the test cell design. The function was two-fold; to hold the test flat against the housing with the desired thermal contact pressure (50 psi) and to provide axial compliance, relieving forces created by the transient thermal gradients brought on by the rapid cooldown process. A molybdenum spacer ring was placed between the wave washers and test flat to uniformly distribute the force on the flat.

6. TEST SET-UP

Due to the cryogenic operating temperatures of the test cell, a thermal isolation adapter was built to isolate the cell from the warm, two axis positioner. The adapter contained posts made from 0.03 inch wall, G-10 fiberglass. Westinghouse manufactures this material in various cylindrical diameters and thicknesses. It is an excellent structural and thermal isolation material. A photograph of the entire assembly can be found in Figure 4. The wires in the photograph connect to thermocouples on both the test flat and cell housing.

The test assembly was placed in a vacuum chamber with a window to allow for real time interferometric testing during the cooldown process. A Zygo interferometer running at 3.39 microns was used in the testing.

7. TEST CELL PERFORMANCE

During the rapid cooling of the test flat, the thermal gradient across the lens element was monitored to correlate the thermal stress experienced by the test flat with the interferograms taken. Refer to the photograph in Fig. 5 for the ambient and cold (<120 K) interferograms. The fringe shift was found to be negligible. In addition, the test cell was instrumented with two thermocouples, one at the center of the flat and the other at the wall of the molybdenum test cell housing. The temperatures of the thermocouples are plotted against time during rapid cooldown in Fig. 6. In Fig. 7, the temperature gradient across the test flat is plotted against time. This plot showed a first peak temperature gradient occurring in the test flat at 100 seconds elapsed time then another sharp peak at 190 seconds after the initiation of cooling. This is the occurrence of the two peak stresses in the test flat. The temperature gradient predicted by the thermal analysis using SINDA is also shown on Fig. 7. The thermal analysis predicted the occurrence of the first peak in temperature gradient but missed the second peak. This is due to the assumption made in the thermal analysis that only a single phase heat transfer would be experienced by the liquid nitrogen coolant whereas, two phase heat transfer was more likely to be experienced by the coolant in the flow channel.

8. LENS CELL DESIGN

The lens cell consists of a brazed housing sub-assembly, lens, spacer, three wave springs, retainer, and aperture stop. Refer to the cross-sectional view in Fig. 8, the exploded isometric illustration in Fig. 9 and the photograph in Fig. 10. The cell housing employed spherical surface lens mounting to maximize contact area and minimize contact stresses.

The housing sub-assembly has three parts; a methane cavity, coolant jacket, and cooling line support. All three parts were machined from molybdenum TZM and brazed together with copper alloy wire. Thermofusion, located in Hayward, CA, performed the brazing process and had key design recommendations. Having an experienced brazing vendor involved in the initial design phase was critical to its success. The housing was manufactured in the following sequence:

1. Rough machined, leaving 0.020/0.030 inches over final dimensions.
2. Heat treated at 2000 F±25 F for one hour in a hydrogen atmosphere.
3. Final machined to the braze dimensions.
4. Furnace brazed per Mil-B-7883, Type II, Grade B.
5. Thermal cycled three times; 300 K to <120 K (80 K).
6. The coolant flow channel was tested with a helium mass spectrometer leak detector.
7. Lens contact surface was ground and polished using test plates to assure the surface radius matched the COLD (120 K) mating germanium lens radius within two fringes at 3.39 microns.

The wave springs were stacked in parallel to apply 55.5 pounds of force (113 psi) on the lens. The molybdenum retainer and brass lens spacer were closely toleranced to preclude any deflection adjustments during assembly. The aluminum aperture stop was fastened to the retainer with screws and spring washers to assure good thermal contact.

The final step in the assembly process was plumbing the two fill/vent coolant lines to the housing. The stainless steel bellows lines were epoxied in place using Epibond epoxy, 1210A/9615-10, manufactured by CIBA-GEIGY Furane Aerospace Products.

9. LENS CELL PERFORMANCE

The lens cell was instrumented with a platinum resistance thermometer (PRT); epoxy mounted onto its molybdenum housing. The volumetric flow rate of the nitrogen coolant was also measured during the test using a mass flow meter. The experimentally measured temperature of the lens cell housing was plotted against time in Figure 11. Since the nitrogen coolant flow rate was measured, this flow rate was used as input to the thermal model to calculate the temperatures of the lens cell housing and the lens itself during rapid cooling. The calculated temperatures are superimposed on the test result in Figure 11 for comparison. From this plot, it is apparent that the temperatures predicted by the thermal model are much higher than the experimental measurement. This indicated that the thermal model is conservative in predicting the performance of the lens cell heat exchanger. The assumption of a single phase fluid flow within the channels of the heat exchanger is too simplistic. Actually, two phase boiling heat transfer in the flow channel was experienced by the liquid nitrogen coolant; enhancing the convection between the liquid and the wall as well as maintaining the nitrogen coolant at its phase changing temperature. The thermal modelling of two phase flow phenomenon is very complex and was not attempted in this study. In summary, the thermal analysis utilized a conservative approach in the thermal design of the lens cell for rapid cooling and the test results were much better than predicted by the thermal model.

10. SUMMARY

This paper has described the processes followed in developing a rapid cooled, infrared lens cell. All operational tests have been successfully completed, demonstrating the lens cell meets all of the original performance requirements.

Under the next phase of the LATS program, Lockheed will design another similar lens cell but with the added feature of phase change material (PCM) containment within the housing. The PCM will allow the cell to be maintained at its operating temperature of 120 K over an extended period. This ability to passively cool lens elements will greatly simplify overall designs of future seekers.

11. ACKNOWLEDGMENTS

The development of this rapid cooled lens cell was performed by the Lockheed Research & Development Division under contract to the U.S. Army. The authors wish to express their gratitude to the LATS program office for the opportunity to work on this challenging assignment. Special thanks goes to Mr. A. Rubero for detailing the final design version and Mr. R. Plummer, the opto-mechanical group leader, for his organizational skills, tenacity and ideas.

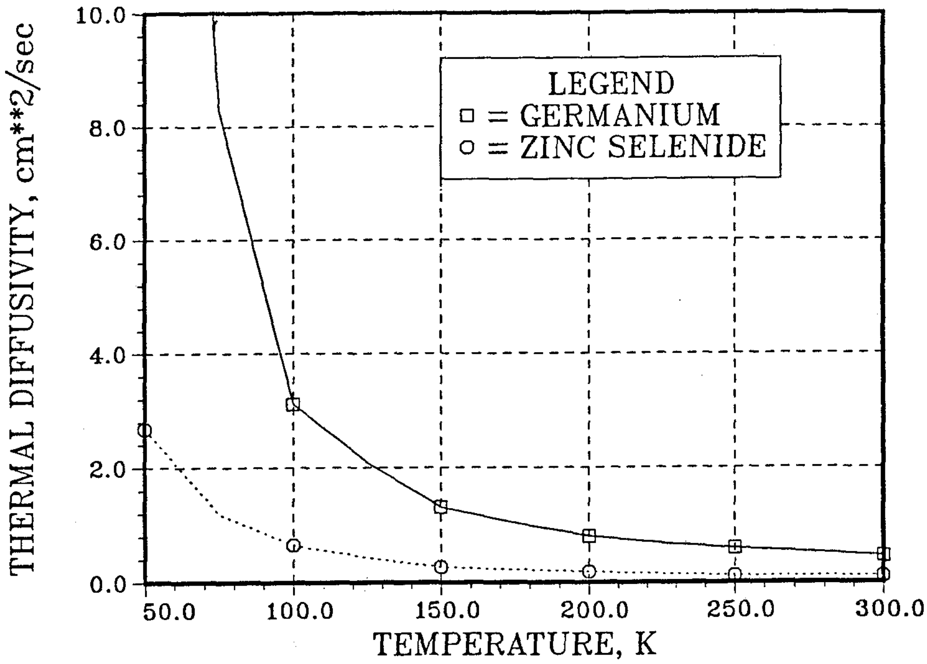

Fig. 1. Thermal diffusivity of germanium and zinc selenide as function of temperature.

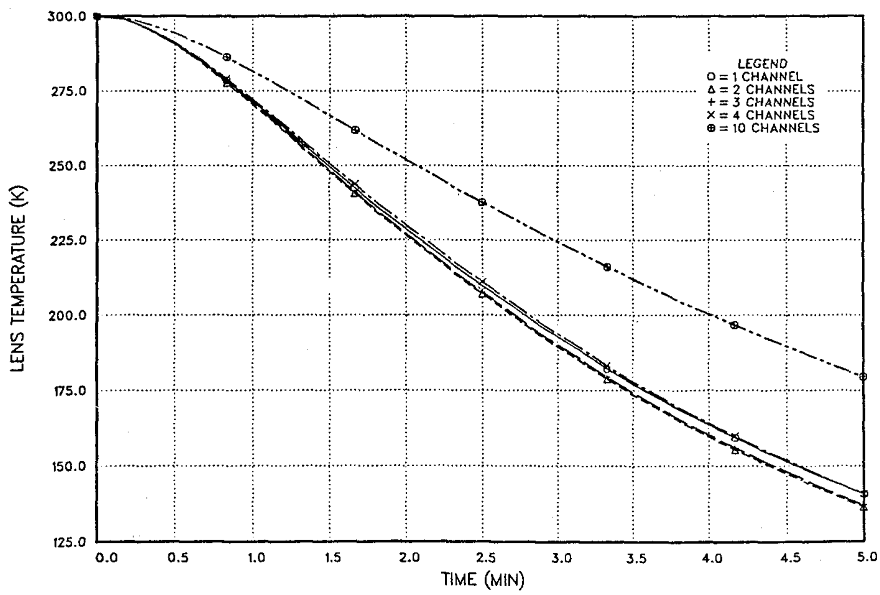

Fig. 2. Parametric study on the effect of the number of flow channels in the lens cell influencing rapid cooling.

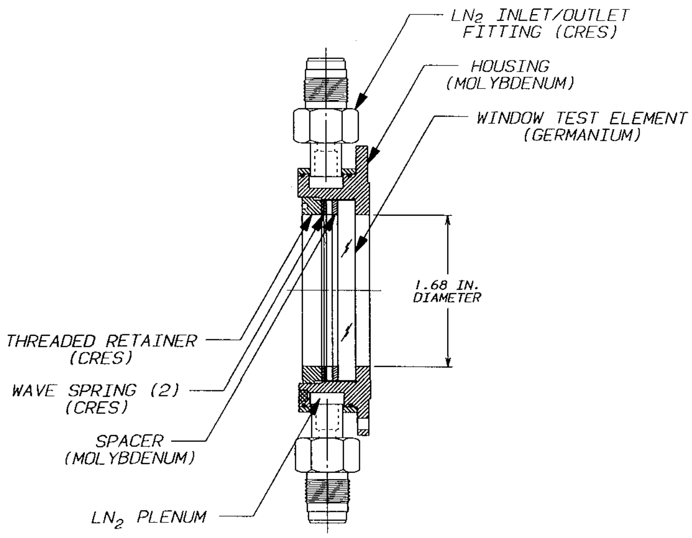

Fig. 3. Test cell cross-section.

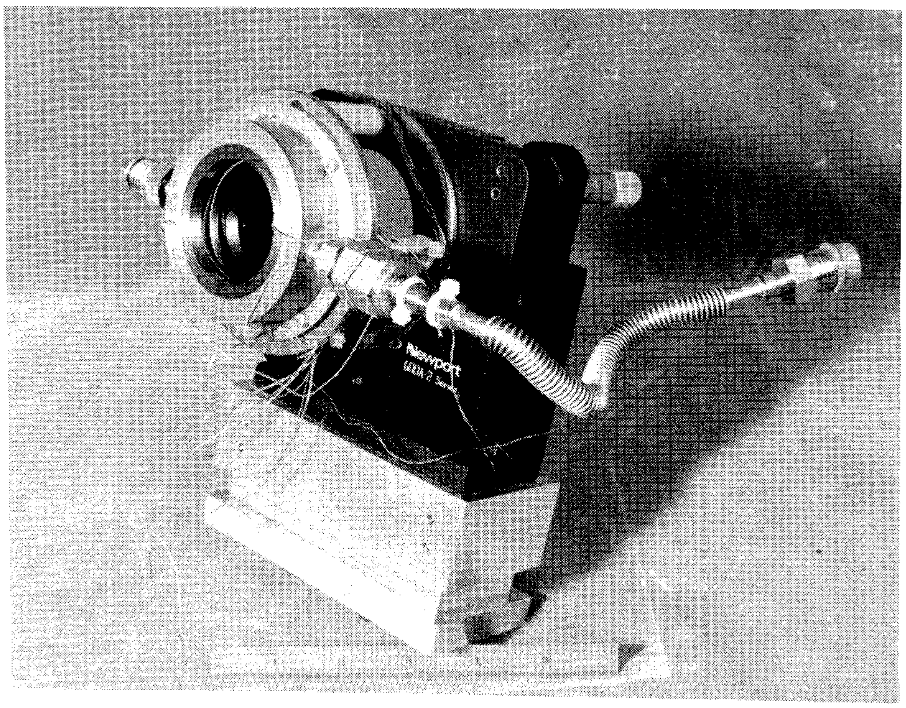

Fig. 4. Instrumented test cell.

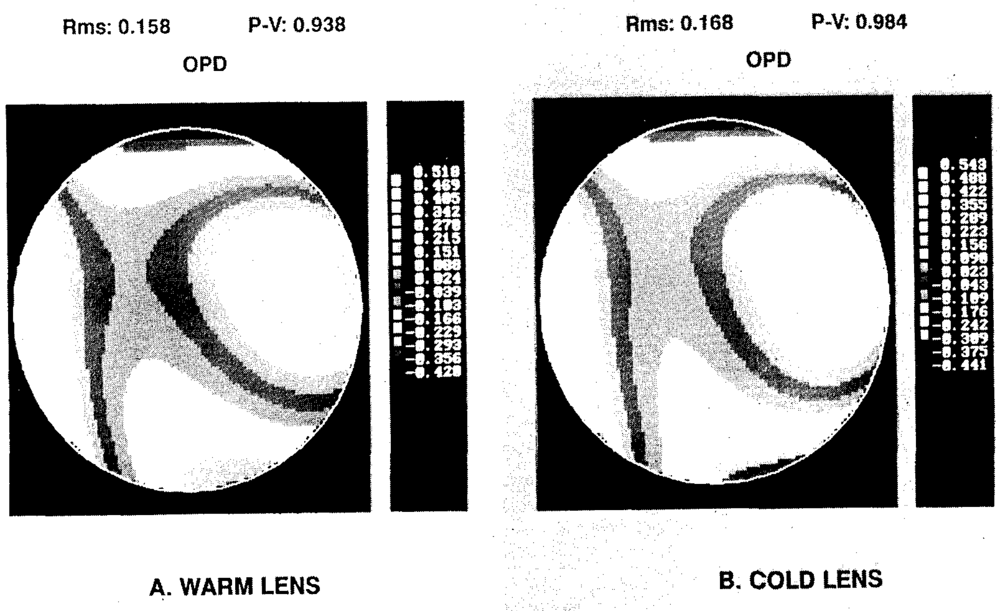

Fig. 5. Test cell interferograms.

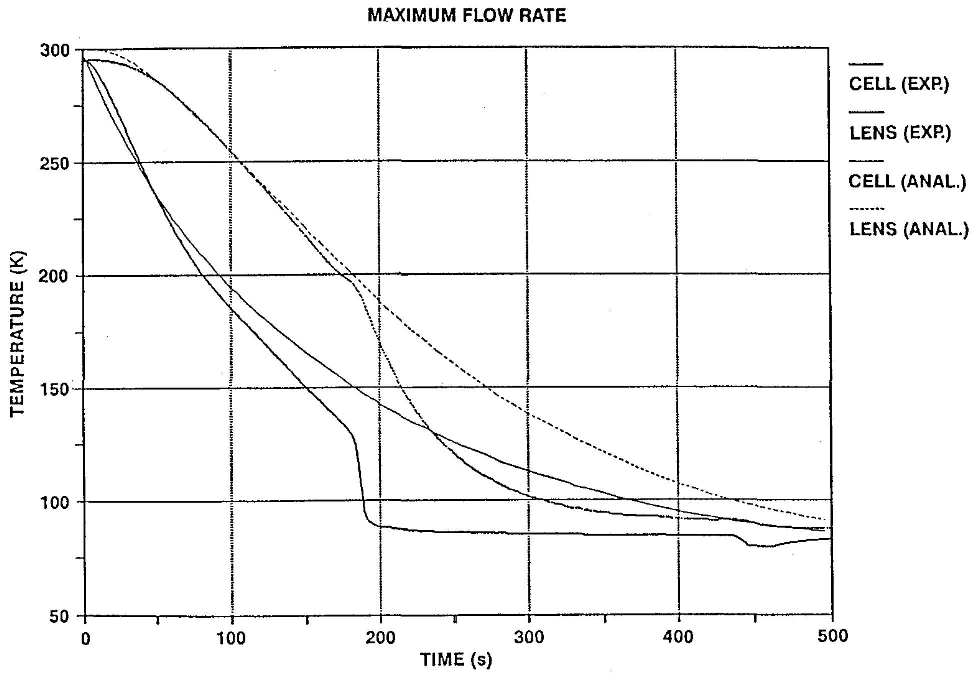

Fig. 6. Temperatures in the test cell during rapid cooling.

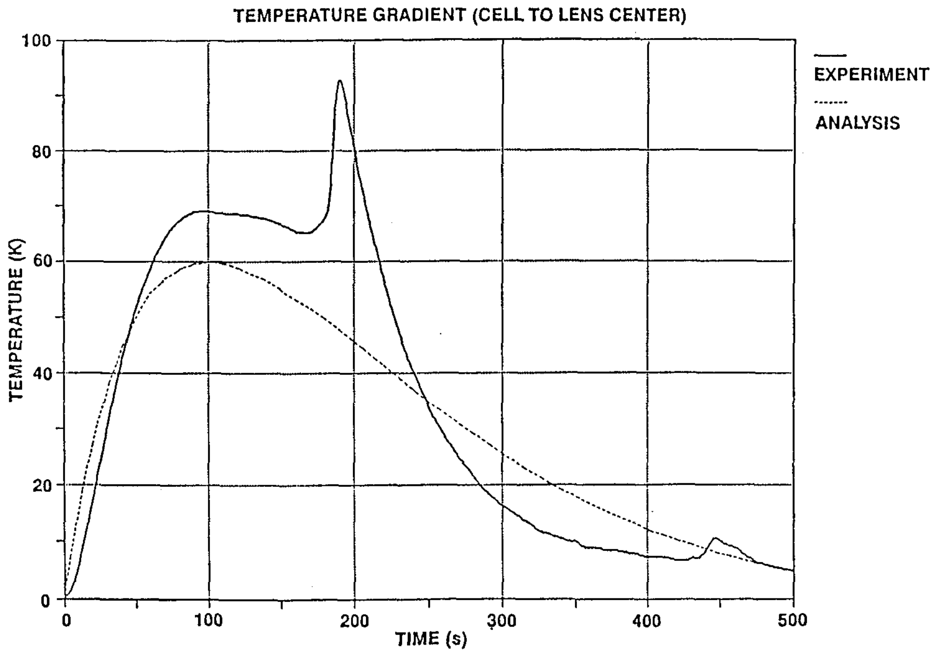

Fig. 7. Temperature gradient in the test cell during rapid cooling.

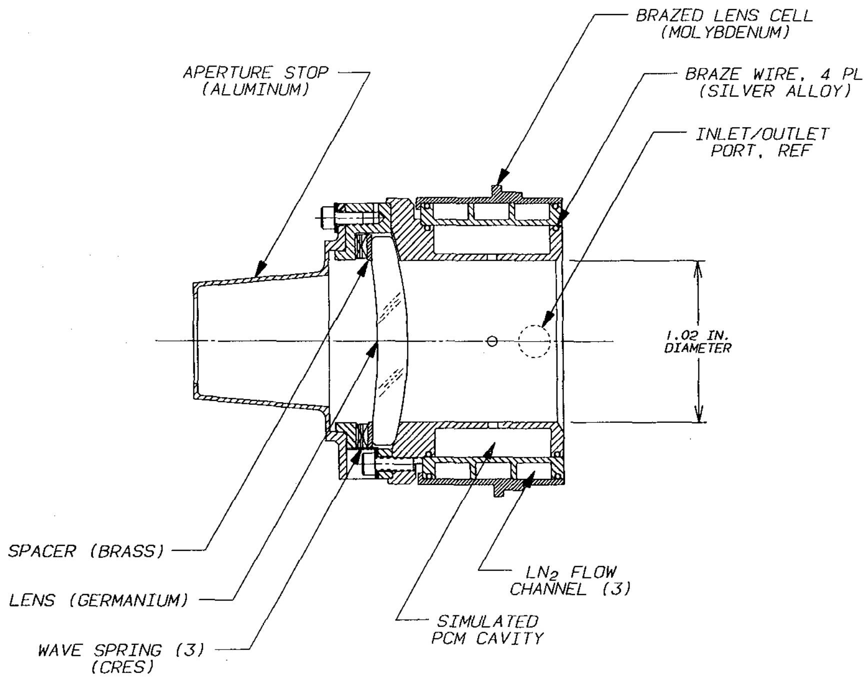

Fig. 8. Lens cell cross-section.

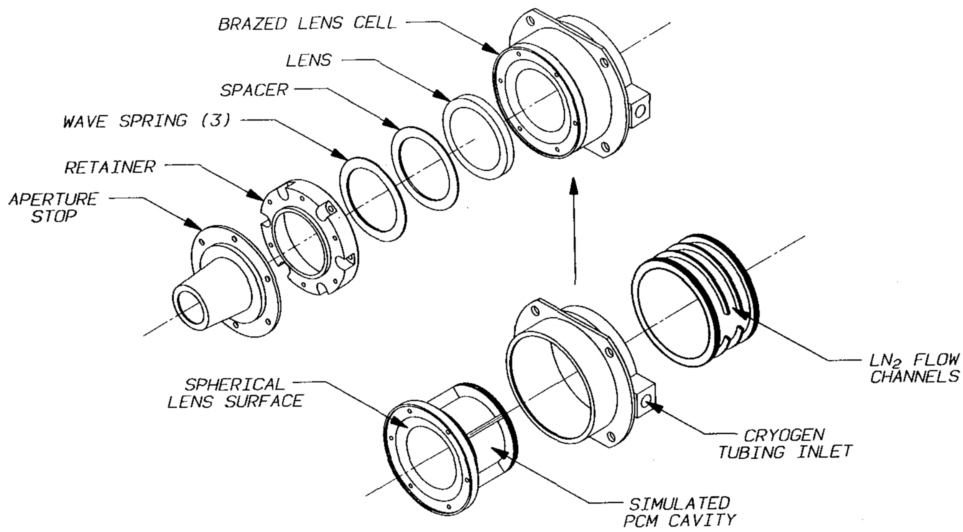

Fig. 9. Lens cell isometric.

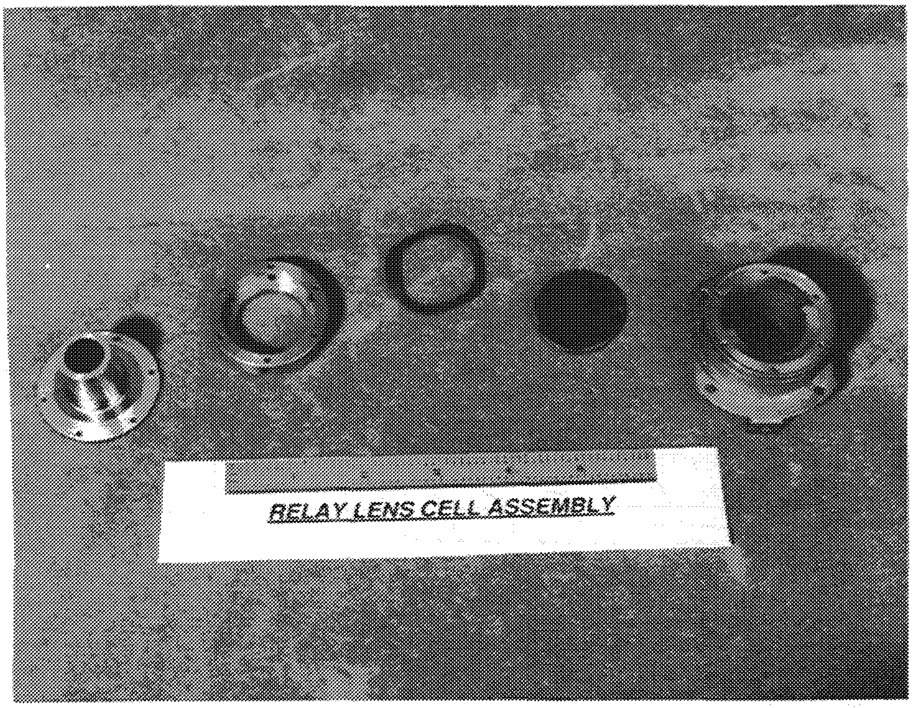

Fig. 10. Lens cell.

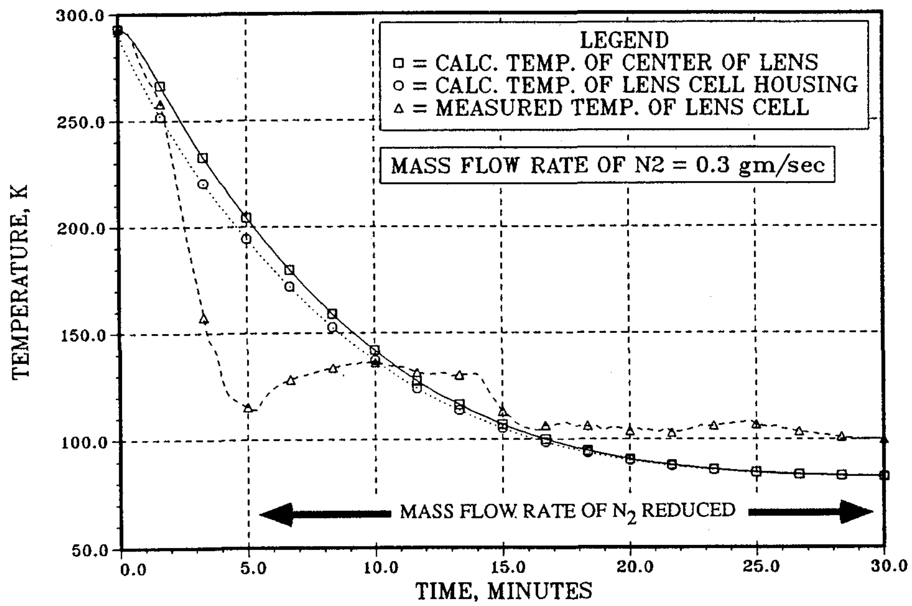

Fig. 11. Measured versus calculated temperatures in the lens cell during rapid cooling.